Comparative Study of Defect Formation in Femtosecond Laser Irradiated Polymers and Crystalline Media

Kallepalli Lakshmi Narayana Deepak[1, 2], Desai Narayana Rao[2]

[1]Aix Marseille Universite, CNRS, LP3 UMR 7341,13288 Marseille, France

[2] School of Physics, University of Hyderabad, Prof. C.R. Rao Road, Hyderabad 500046, India

kallepalli@lp3.univ-mrs.fr; dkln1982@gmail.com

Abstract

Herein, we present and compare our spectroscopic results on femtosecond (fs) laser irradiated polymers Poly Methyl Methacrylate (PMMA), Poly Di Methyl Siloxane (PDMS) with crystal media such as Lithium Niobate ($LiNbO_3$). Dependence of the structure width with irradiation dose and scan speed is illustrated. Keldysh parameter calculations are highlighted to describe the dominant ionization process. Formation of micro-craters at low irradiation dose and high scan speed is analyzed through minimal pulse to pulse overlap. Formation of defects such as optical and paramagnetic centers in case of polymers is compared with the absence of such defects in crystal media. Confocal micro-Raman studies carried out on polymers and crystal are presented.

Keywords

Fs laser direct writing; Polymers; Crystals; Emission; Defects

Introduction

Fs laser direct writing is a unique tool for fabrication of micro and nano-structuration of transparent materials as it provides short pulse duration but at the same time sufficient fluence to overcome the damage threshold of the targets [1]. Since the interaction of these fs pulses with transparent material is nonlinear, the energy deposited by a focused fs pulse is confined inside the focal volume. This results in a sub-micrometer structuring of materials which finds application in various fields [2-9]. A variety of materials including metals, dielectrics, polymers, and semiconductors have been successfully processed by with fs pulses [10-15].

Experimental Results

Bulk samples of PMMA were purchased from Goodfellow, USA. PDMS was home made. These samples were cut into 1 cm × 1 cm dimensions and sides were polished. X cut $LiNbO_3$ was used in our experiments. Before microfabrication experiments were carried out, these samples were sonicated in distilled water to remove unwanted dust. Microstructures, and 2-dimensioal grids (for ESR analysis) were fabricated using a Ti: sapphire oscillator amplifier system operating at a wavelength of 800 nm delivering ~100 fs pulses, ~1 mJ output energy pulses with a repetition rate of 1 kHz. The near-transform nature of the pulses was confirmed from the time-bandwidth product. Three translational stages (Newport) were arranged three dimensionally to translate the sample in X, Y, and Z directions. Laser energy was varied using the combination of half wave plate and a polarizer. We have used 40X (Numerical Aperture (NA) of 0.65) and 20X (NA of 0.4) microscope objectives in our experiments for focusing.

Three different sets of experiments were performed using 40X microscope objective. In set 1, structures were fabricated at 1 mm/s speed while in set 2, structures were fabricated at 0.5 mm/s speed. In set 3, energy used was kept constant while the scanning speed was changed. All these three sets were carried out below 300 μm from the surface of the $LiNbO_3$ X-cut crystal using 40X microscope objective lens. Figures 1 (a) and 1 (b) show the confocal microscope images of two structures fabricated at 100 μJ, and 50 μJ energies at 1 mm/s speed using 40X microscopic objective lens. As it can be seen clearly, the structures fabricated become smoother and narrower at low energies (fluences). Only central portion of the incident fs laser Gaussian pulse leads to damage of the material as the fluence exceeds the damage threshold of the material. This aspect is clearly depicted from the confocal microscope images depicted in Figure 1.

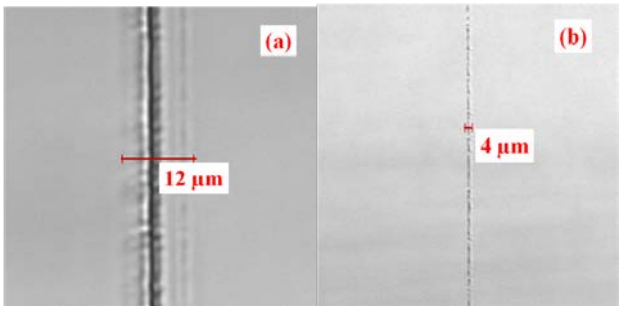

FIG. 1 CONFOCAL MICROSCOPE IMAGES OF A STRUCTURE FABRICATED WITH 1 MM/S SPEED WITH 40X MICROSCOPE OBJECTIVE LENS AT ENERGY OF (A) 100 µJ (B) 50 µJ

Figure 2 (a) shows the confocal microscope image of structures fabricated at different energies with 0.5 mm/s speed. Figure 2 (b) shows a confocal microscope image of a structure fabricated at 635 nJ energy. From figure 2 (a), it can be inferred that there is a reduction in structure width with decrease in energy. Structures fabricated at low energies were found to be smooth as indicated in figure 2 (b). Structure widths and energies used for fabricating set 1 and set 2 are plotted in figure 2 (c). An increment in structure width is found with energy in each set and structures fabricated in set 2 with scanning speed 0.5 mm/s are found to be having more width when compared with set 1 at the same energy. As scanning speed is reduced, material is exposed to the laser for a longer period leading to an increase in the structure width.

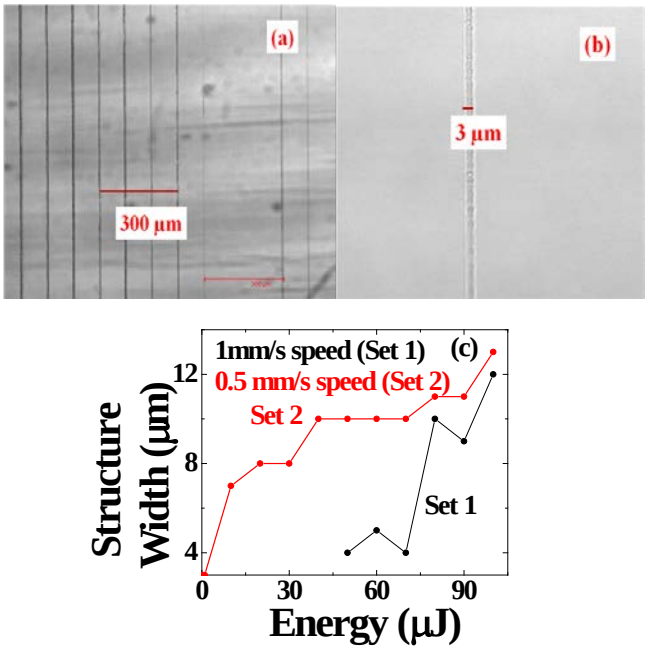

FIG. 2 CONFOCAL MICROSCOPE IMAGE OF (A) MICROSTRUCTURES FABRICATED AT 0.5 MM/S SPEED. LEFT EXTREME STRUCTURE IS FABRICATED AT 100 µJ ENERGY. LEFT TO RIGHT, ENERGY IS DECREASING. SPEED IS 0.5 MM/S. (B) THE STRUCTURE FABRICATED AT 635 NJ ENERGY. (C) PLOT OF STRUCTURE WIDTH VERSUS ENERGY FOR SET 1 AND SET 2.

Figure 3 (a) shows confocal microscope images of set 3 structures fabricated at a particular energy of 40 µJ with different writing speeds as 0.1, 0.2, 0.5, 0.8, 1, 2, 4, 6, 8 and 10 mm/s (from left to right). Figure 3 (b) shows confocal microscope image of a structure fabricated at 4 mm/s speed, which clearly shows the formation of pearl like structure (formation of microcraters). This phenomenon was observed from 2 mm/s speed to higher scanning speeds. There is monotonous decrease in structure width with increasing writing speeds. Formation of 'pearl like' structure can be attributed to the reduction in number of incident pulses on the material at higher writing speeds as pulse to pulse overlap is minimal at higher scanning speeds. Figure 3 (c) shows a plot of structure width with scanning speed of the translation stage. Structure width can be changed by either continuous modifications or a chain of pulses depending on energy and scan speeds. From figure 3 (c), it is clear that structure width starts decreasing at high scan speeds as exposure at a spot in the material is reduced. Similar structures were also fabricated in PMMA and PDMS polymers.

The bandgap of $LiNbO_3$ is 3.75 eV [16-17] and for PMMA and PDMS, it is 4.58 and 2-2.84 respectively [18-19]. Since the polymers (PMMA and PDMS) and LNB crystal under investigation are transparent to UV-Visible light, we cannot process these materials by linear absorption mechanisms. Also these materials do not posses any absorption in near IR around 800 nm wavelengths that we used to fabricate the structures. Each 800 nm photon carries 1.55 eV energy. This implies that nonlinear absorption process is an essential tool to create modification in these materials. Minimum three photons are required for modification of these materials. As 800 nm lasers is focused to a spot size of 1.5 and 2.44 µm respectively for 40X and 20X objective lenses, it is easy to achieve nonlinear modification in these materials. In addition to the three photon absorption process, Keldysh parameter is used to estimate the dominant mechanism responsible for ionization process [20-23]. In the present study, it is tunneling ionization which is mainly responsible for the modification process as Keldysh parameter is less than 1.5 [20-21]. Figure 3 (d) shows the plot of peak intensity versus Keldysh parameter. Peak intensities are calculated for energies ranging from 0.46-100 µJ. For all these energies, Keldysh parameter is still less than 1.5. The fabricated structures in LNB crystal were found to be having less width when compared with polymers as polymers are soft compared with crystals.

Also, the inorganic crystalline materials have higher damage thresholds. The ablation threshold of the lithium niobate crystal is 3.92 J/cm² [24] for single shot.

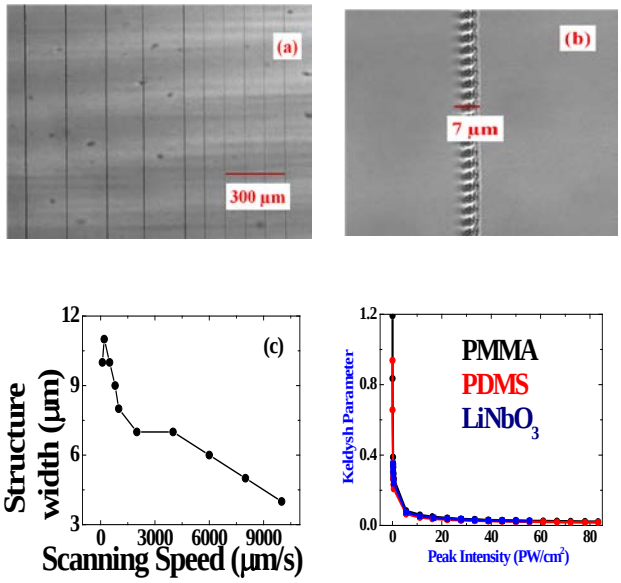

FIG. 3 (A) CONFOCAL MICROSCOPE IMAGE OF MICROSTRUCTURES FABRICATED AT DIFFERENT SCAN SPEEDS WITH 40 µJ ENERGY. LEFT EXTREME STRUCTURE IS FABRICATED AT 0.1 MM/S SPEED. (B) PEARL LIKE STRUCTURE FABRICATED AT 40 µJ ENERGY, 4 MM/S SPEED. (C) PLOT OF STRUCTURE WIDTH WITH SCANNING SPEED. (D) PLOT OF KELDYSH PARAMETER WITH PEAK INTENSITY

Interestingly, we found formation of various defects in these materials due to polymer chain breaking in polymer systems and formation of defect sites due to voids in case of lithium niobate (LNB) crystal. We found emission coming from the fabricated structures of polymers. Figure 4 (a) shows one of the structures fabricated in PMMA. In order to record emission, we fabricated gratings over a large area in PMMA and PDMS. Closely spaced lines were fabricated in PMMA using 40X microscope objective lens with energy of 10 µJ, speed 1mm/s, period 30 µm and in case of PDMS the energy used was 50 µJ with scan speed of 1 mm/s and the period of 10 µm. Figure 4 (b) shows the peak shift in PMMA with the excitation wavelength. This indicates that myriad optical centers were generated and suitably few particular optical centers were excited depends upon excitation wavelength used. Figure 4 (c) shows the excitation spectra at different monitoring wavelengths. Though one would expect shift in the excitation spectra, they all look similar. This is logical as all the optical centers formed are from the same monomer unit. The maximum absorption is around 367 nm which is ascribed as due to n → π* transition. These results were reported by our group earlier [25-34]. Similar studies are carried out in case of LNB crystal also. However, we have not observed any optical centers when excited in the visible spectrum. Most of the polymers contain active groups such as aldehyde, ketone groups etc which are responsible for the observation of emission after absorption. Absence of such active groups in crystalline media could be one reason for absence of emission after they are treated with fs pulses.

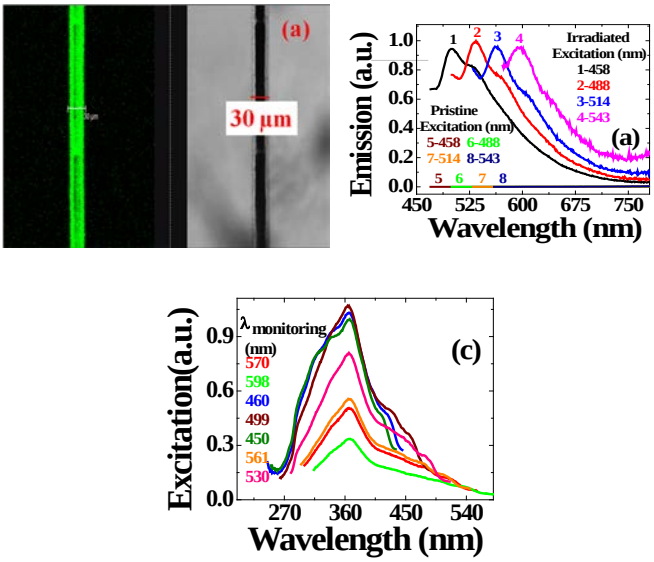

FIG. 4 (A) CONFOCAL MICROSCOPE IMAGES OF PMMA (GOODFELLOW). ~20 µM WIDE MICRO CHANNEL INSIDE THE BULK OF PMMA. (B) EMISSION SPECTRA AT DIFFERENT EXCITATION WAVELENGTHS (C) EXCITATION SPECTRA AT DIFFERENT MONITORING WAVELENGTHS

Similar studies were extended to PDMS polymer also. Unlike PMMA polymer, we noticed sharp peaks with emission background as shown in figure 5 (a) with similar excitation spectra at different monitoring wavelengths depicted in figure 5 (b). Upon careful investigation, we found that the same PDMS polymer did not show any sharp peaks for excitation wavelengths below 400 nm. This is due to the matching of Raman modes with the emission bands. In case of PDMS, the excitation wavelengths at 300, 420, 440 nm gave Raman peaks of PDMS with Raman mode of 3106 cm^{-1} which is CH stretching vibration mode [35]. Also excitations at 363, 458, 488, 514, 543 nm gave two Raman modes of PDMS at 2907, and 2965 cm^{-1} which are CH_3 symmetric and asymmetric stretch modes [36]. Also, compared with PMMA, it is very clear in PDMS that sharp peaks appear on broad emission background which indicates the component of emission along with Raman signal. In the literature, researchers have reported red edge effect [37-46] which is prominent in the case of polymers and this could be the main phenomena for the shift of emission

peak with the excitation wavelength. As these polymers were irradiated, different chemical moieties or species or defect centers were formed due to polymer chain breaking and these defects exhibited red edge effect. Figure 5 (c) shows the plot of emission peak as a function of excitation wavelength for fs laser irradiated PMMA and PDMS. Also the role of transitions involved within the functional groups or active groups cannot be ignored as stated earlier. Figure 5 (d) represents a schematic involved in possible transitions involved within these groups.

Apart from the presence of optical centers which are emissive, we also have examined the samples using electron spin resonance spectrometer (ESR) for the presence of

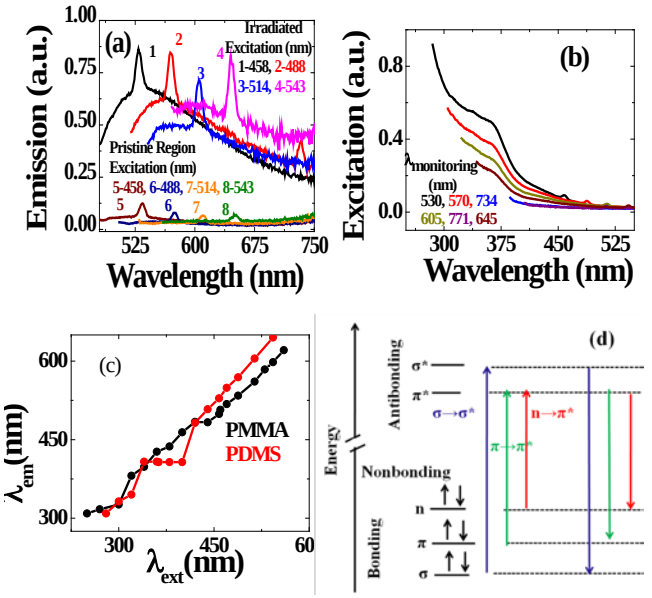

FIG. 5 (A) EMISSION SPECTRA OF FS LASER IRRADIATED PDMS AT DIFFERENT EXCITATION WAVELENGTHS (B) EXCITATION SPECTRA COLLECTED AT DIFFERENT MONITORING WAVELENGTHS FOR FS LASER IRRADIATED PDMS (C) PLOT OF RED EDGE EFFECT IN PMMA AND PDMS (D) SCHEMATIC REPRESENTATION OF POSSIBLE TRANSITIONS IN FUNCTIONAL GROUPS

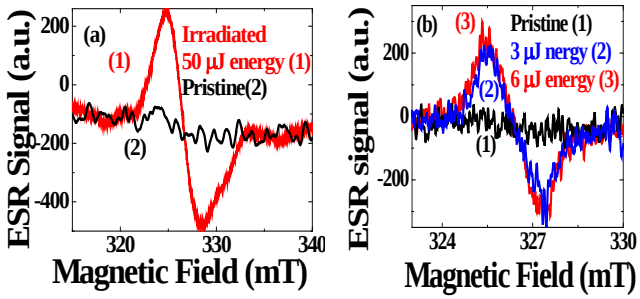

FIG. 6 (A) ESR SPECTRUM OF IRRADIATED PMMA AT 50 μJ ENERGY, 1MM/S SPEED. (B) ESR SPECTRUM OF IRRADIATED PDMS AT 3, AND 6 μJ ENERGY AND A SPEED OF 1 MM/S

paramagnetic defects. As pristine polymers are diamagnetic they did not show presence of any free radicals. Irradiated regions of PMMA and PDMS polymers showed ESR signal at the same magnetic field of 326 mT with **'g'** value of 2 from which we predict the existence of peroxide type free radicals. PMMA illustrated decrease in ESR signal in few days of time while the PDMS showed ESR signal even after six months indicating that the free radicals are stable in this polymer. Here, the role of defects responsible for emission on paramagnetism is interesting. But, we found that the emission from the irradiated regions of polymers explained earlier did not vanish even one year after the exposure. This clearly suggests that the free radicals which contributed to ESR signal do not lead to the emission except in the case of PDMS. As in the case of PDMS, since we observed ESR signal even after several months, it may be possible that the same radicals exhibited the behaviour of emission also along with paramagnetism. Graubner et. al has treated PDMS with 172 nm irradiation. They reported the abstraction of hydrogen (which is initial step) followed by reaction of methylene radicals with oxygen leading to peroxy radical formation. This peroxide radical rearranges to silanol group. We strongly feel that the silanol group is mainly responsible for its stability for long time [47]. Nie et al. [48] have reported typical characteristic 9 line spectrum of PMMA immediately after fs laser irradiation. However, our data depicted a single peak in the ESR spectra for PMMA, and PDMS since the experiment/irradiation was carried out in the atmospheric environment and at room temperature. Figure 6 (a) and 6 (b) show the same results in fs laser irradiated PMMA and PDMS.

To carry out ESR analysis in case of LNB crystal, we fabricated gratings underneath and on the surface of the lithium niobate crystal. Energy used was 100 μJ with 40 X microscope objective and 1 mm/s as the scanning speed. Grating structure has 20 μm period in between lines. In case of polymers we observed paramagnetic radicals in all orientations of the sample with respect to the direction of magnetic field (Parallel, Perpendicular and 45°). Since the properties of the crystals are anisotropic due to symmetry involved in the crystal structure, we observed orientation dependent ESR signal. Interestingly, pristine LNB crystal has also shown ESR signal when sample was (what crystal axis) oriented parallel to the magnetic field direction. Several reasons such as existence of defects, oxygen vacancies etc were reported earlier by

several groups that contribute towards ESR signal for pure LNB crystal [49]. Figure 7 (a) shows the ESR signals in three different orientations of the crystal with respect to the direction of magnetic field applied. Only parallel orientation of the crystal with respect to the magnetic field has shown the existence of paramagnetic radicals. Figure 7 (b) shows the results obtained with irradiated sample (for buried grating). Similar results were obtained, since the irradiated crystal also contains maximum volume of pure crystal, It has exhibited ESR signal in parallel configuration. Figure 7 (c) compares ESR signals of irradiated and unirradiated samples in parallel configuration.

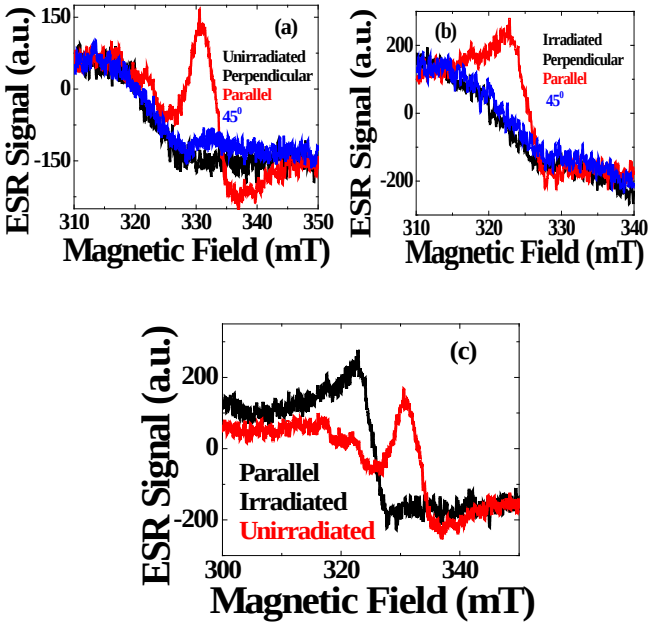

FIG. 7 ESR SIGNAL OF (A) UNIRRADIATED PURE LNB CRYSTAL IN DIFFERENT ORIENTATIONS (B) UNIRRADIATED PURE LNB CRYSTAL IN DIFFERENT ORIENTATIONS (C) IRRADIATED AND PURE CRYSTALS IN PARALLEL ORIENTATION

We recorded confocal micro-Raman spectra also for fs laser irradiated polymers and LNB crystal. Figure 8 (a) and 8 (b) show the Raman spectra collected in different regions of the fabricated structures at high and low energies. Figure 8 (a) shows the Raman spectra recorded for a grating structure fabricated in PMMA with 50 μJ, 0.25 mm/s speed using 40X NA objective lens. Figure 8 (b) shows Raman spectra collected from a PMMA grating fabricated at ~3 μJ energy with 500 μm/sec scanning speed with 0.65 NA (40X) objective lens. The bands in the region of 2800-3200 cm^{-1} correspond to vibrational bands of O-CH_3 and α–CH_3 [50-51]. We recorded Raman spectra in the central portion and edge portion of the structure to compare with pristine regions of the polymer. In case of structures fabricated at high energies, we noticed peak broadening which is an indication of the formation of defects which could be optical centers and/or paramagnetic centers.

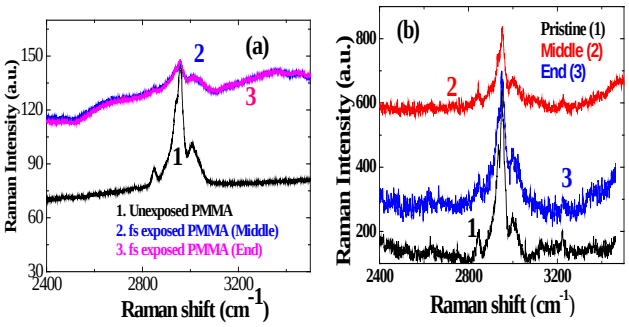

FIG. 8 (A) RAMAN SPECTRA FROM A PMMA GRATING (50 μJ, 0.25 MM/S) WITH THE BOTTOM CURVE REPRESENTING THE SPECTRUM COLLECTED FROM UNMODIFIED REGIONS OF PMMA WHILE THE MIDDLE AND TOP CURVES FROM THE FS MODIFIED REGIONS. (B) MICRO-RAMAN SPECTRUM OF PMMA GRATING (~3 MJ, 500 MM/SEC) ACHIEVED WITH 0.65 NA (40X) OBJECTIVE. THE CURVES HAVE BEEN SHIFTED FOR CLARITY. INSET SHOWS THE REGIONS FROM WHICH THE SPECTRA ARE COLLECTED

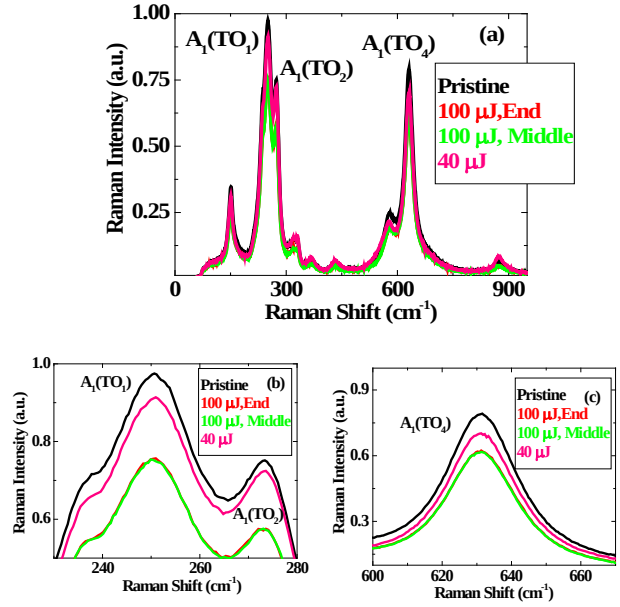

FIG. 9 (A) RAMAN PLOTS OF PRISTINE LNB AND MODIFIED REGIONS OF LNB (B): ENLARGED MODES OF $A_1(TO_1)$ AND $A_1(TO_2)$ (C): ENLARGED RAMAN MODES OF $A_1(TO_4)$

We carried out Raman analysis for the fabricated structures in LNB crystal. There were three main transverse optical phonon modes reported in the literature [52-59]. Figure 9 (a) shows the three phonon modes $A_1((TO_1)$, $A_1((TO_2)$, and $A_1((TO_4)$. $A_1((TO_1)$ phonon mode corresponds to the motion, along the z axis, of Ni ions against the O sub-lattice, while Li ions remain relatively static [56]. This mode is considered to be important and more sensitive to changes in Nb

sub-lattice. Spectral broadening and low frequency shifting can determine the Li/Nb content as Li content is locally reduced [54, 56-58]. $A_1((TO_2)$ mode is related to displacements along z axis between Li and Nb ions while the O ions are stationary [54]. $A_1((TO_4)$ mode corresponds to distortions of the octahedral only in xy plane. This mode has high relevance in assessing the compactness, and hence refractive index changes [52, 54-56]. Raman spectral analysis is a powerful technique for the detection of local modifications in chemical composition, unit cell volume, ionic displacement, local disorder, and defects. We adapt some of the mechanisms leading to changes in Raman modes from the references found in [52-61]. Table 1 shows various mechanisms and the Raman modes response in lithium niobate crystal.

S. No.	Mechanism	Raman mode response	Reference
1	Local environment densification and compressive stress	Increase in phonon mode frequencies especially for $A_1((TO_4)$	58
2	Reduction in the Li content	Broadening of Raman modes especially for $A_1((TO_1)$ and Raman shift for $A_1((TO_1)$	54, 56-57
3	Reduction in spontaneous polarization due to large-scale defects	Broadening of Raman modes and Reduction in Raman intensity	59-61
4	Ionic rearrangement	Changes in Raman shifts	54,60

We fabricated several structures in LNB crystal and carried out Raman analysis. Figure 9 (a) shows the Raman modes of LNB crystal. We collected Raman spectra for a structure fabricated at 100 μJ energy in middle and end regions and also for a structure fabricated at 40 μJ energy with 0.5 mm/s scanning speed and using 40X objective. In order to analyse the Raman modes, we enlarged figure 9 (a) and plotted in figure 9 (b) which shows the changes in Raman intensities of $A_1(TO_1)$ and $A_1(TO_2)$ modes. Though there is a slight shift of 1 cm^{-1} for the structure fabricated at 100 μJ with pristine region, it cannot be accounted for reduction in the Li content as the spectral resolution of the instrument we used is ±1 cm^{-1}. These results show that there is only Raman intensity change from figures 9 (b) and 9 (c). This could be due to lattice deformity leading to creation of defects.

From the Raman spectra recorded for pristine and modified regions, we observe a decrease in the Raman intensity for all the three transverse optical phonon modes which could be due to the formation of defects and voids because of large intensities associated with high energy fs pulses. However, these defects did not exhibit properties of emission like optical centers in polymer media and para-magnetism described earlier.

Conclusions

We reported spectroscopic properties of fs laser irradiated polymers and LNB crystal. In case of polymers we observed emission from the fs laser modified regions and it is found to be shifting with the excitation wavelength due to various transitions involved in functional groups and red edge effect. Also these materials exhibited paramagnetism upon fs laser irradiation unlike LNB crystal. Confocal micro-Raman studies revealed broadening in case of polymers which is an indication of the presence of radicals and or defects which are confirmed through emission and ESR studies. Fs laser irradiated LNB crystal also showed the presence of defects but they do not exhibit the properties of emission and paramagnetism (like polymer media) due to absence of functional groups.

ACKNOWLEDGMENT

KLND acknowledges CSIR for his fellowship. DNR acknowledges funding from RCI, Hyderabad.

REFERENCES

A. Bajorek, and J. Paczkowski, "Influence of the attachment of chromophores to a polymer chain on their twisted intramolecular charge transfer in dilute solution," Macromolecules Vol.31, 86-95, 1998.

A. Baum, P. J. Scully, W. Perrie, D. Jones, R. Issac, and D. A. Jaroszynski, "Pulse-duration dependency of femtosecond laser refractive index modification in poly(methyl methacrylate),"Opt. Lett. Vol. 33, 651-653, 2008.

A. C. Tien, S. Backus, H. kapteyn, M. Murnane, and G. Mourou, "Short-Pulse Laser Damage in Transparent

Materials as a Function of Pulse Duration,"Phys. Rev. Lett. Vol. 82, 3883-3886, 1999.

A. Datta, S. Das, D. Mandal, S. K. Pal, and K. Bhattacharyya, "Fluorescence monitoring of polyacrylamide hydrogel using 4-aminophthalimide, "Langmuir Vol. 13, 6922-6926, 1997.

A. Jayaraman, and A. A. Ballman, "Effect of pressure on the Raman modes in LiNbO3 and LiTaO3," J. Appl. Phys. Vol. 60, 1208-1212, 1986.

A. N. Rubinov, and VI Tomin, Opt. Spektr. 1970;29;1082-1086.

A. Royon, Y. Petit, G. Papon, M. Richardson, and L. Canioni, ¨Femtosecond laser induced photochemistry in materials tailored with photosensitive agents [invited],¨ *Opt. Mat. Exp.* Vol. 1 (5), pp. 866-882, 2011.

Airan Rodenas, Amir H. Nejadmalayeri, Daniel Jaque, and Peter Herman, "Confocal Raman mapping of optical waveguides in LiNbO3 fabricated by ultrafast high-repetition rate laser-writing," Opt. Exp. 16, 13979-13989.

Alexander P. Demchenko, "The red-edge effects: 30 years of exploration," Luminescence Vol. 17, 19-42, 2002.

Andrew J. Lovinger; Don D. Davis, Frederic C. Schilling, Frank J. Padden, Jr., and Frank A. Bovey, John M. Zeiglert, Solid-state Structure and Phase Transitions of Poly (dimethylsilylene), Macromolecules, Vol. 24, 132-139, 1991.

B. C. Stuart, M. D. Feit, S. Herman, A. M. Rubenchik, B. W. Shore, and M. D.Perry, "Nanosecond-to-Femtosecond Laser-Induced Breakdown in Dielectrics,"Physical Review B-Condensed Matter Vol. **53**, 1749-1761, 1996.

C. A. Merchant, J. S. Aitchison, S. GarciaBlanco, C. Hnatovsky, R. S. Taylor, F. Agullo Rueda, A. J. Kellok, and J. E. E. Baglin, "Direct observation of waveguide formation in KGd(WO4)2 by low dose H+ ion implantation," Appl. Phys. Lett. Vol. 89, 111116, 2006.

C. Thierfelder, S. Sanna, Arno Schindlmayr, and M. G. Schmidt, "Do we know the bandgap of lithium niobate," Phys. status Solidi C Vol. 7, No. 2, 362-365, 2010.

D. W. Mayo, F. A. Miller, and R. W. Hannah, "Course Notes on Interpretation of Infrared and Raman spectra," Wiley Interscience, 2003

D. W. Mayo, F. A. Miller, R. W. Hannah, Course Notes on Interpretation of Infrared and Raman spectra, Wiley Interscience, 2003.

E. N. Glezer, M. Milosavljevic, L. Huang, R. J. Finlay, T.-H. Her, J. P. Callan, and E. Mazur, "Three-dimensional optical storage inside transparent materials," Opt. Lett. Vol. 21(24), 2023–2025, 1996.

F. Abdi, M. Aillerie, P. Bourson, M. D. Fontana, and k. Polgar, "Electro-optic properties in pure LiNbO3 crystals from the congruent to the stoichiometric composition," J. Appl. Phys. Vol. 84, 2251-2254, 1998.

F. K. Christensen, M. Mullenborn, "Sub-band-gap laser micrpmachining of lithium niobate," Appl. Phys. Lett.Vol. 66 (21), 2772-2773, 1995.

G. Della Valle, R. Osellame, and P. Laporta, "Micromachining of photonic devices by femtosecond laser pulses," J. Opt. A: Pure Appl. Opt. Vol. 11, 013001, 2009.

G. Della Valle, R. Osellame, and P. Laporta, "Micromachining of photonic devices by femtosecond laser pulses," J. Opt. A: Pure Appl. Opt. Vol. 11, 013001, 2009.

H. Lao, H. Zhu, and X. Chen, "Surface Ablation of Congruent and Mg-Doped Lithium Niobate by Femtosecond Laser," ISSN 1054-660X, Laser Physics, 1-5, 2009.

H.-B. Sun, Y. Xu, S. Matsuo, and H. Misawa, "Microfabrication and characteristics of two-dimensional photonic crystal structures in vitreous silica," Opt. Rev. Vol. 6(5), 396–398, 1999.

I. Savova, I. Savatinova, and E. Liarokapis, "Phase composition of z-cut protonated $LiNbO_3$:a Raman study, " Opt. Mat. Vol. 16, 353-360, 2001.

J Qiu, K Miura, and K Hirao, "Femtosecond laser-induced micro features in glasses and their applications. Journal of Non-Crystalline Solids," Vol. 354, 1100–1111, 2008.

J. B. Birks, "Photophysics of Aromatic molecules," Wiley-Inter-science: London 1970.

J. Burghoff, H. Hartung, S. Nolte and A. Tunnermann, "Structural properties of femtosecond laser-induced modifications in LiNbO3," Appl. Phys. A Vol. 86, 165-170, 2007.

J. Qiu, K. Miura, and K. Hirao, "Femtosecond laser-induced micro features in glasses and their applications," Journal of Non-Crystalline Solids, Vol. 354, 1100–1111, 2008.

K. A. Al-Hassan, and M. A. El-Bayoumi, "Large edge-excitation red shift for a merocyanine dye in poly (vinyl alcohol) polymer matrix," J. Polymer Sci. B, Vol. 25, 495-500, 1987.

K. A. Al-Hassan, and T. Azumi, "The red edge effect as a tool for investigating the origin of the anomalous fluorescence band of 9,9′-bianthryl in rigid polar polymer matrices," Chem. Phys. Lett. Vol. 150, 344-348, 1988.

K. A. Al-Hassan, and W. Rttig, "Free volume sensing fluorescent probes," Chem. Phys. Lett. Vol. 268, 110-116, 1997.

K. J. Thomas, M. Sheeba, V P N Nampoori, C P G Vallabhan, and P Radhakrishnan "Raman spectra of polymethyl methacrylate optical fibres excited by a 532 nm diode pumped solid state laser" J. Opt. A: Pure Appl. Opt. Vol. 10, 055303 (5pp), 2008.

K. L. N. Deepak, D. Narayana Rao, and S. Venugopal Rao, "Fabrication and optical characterization of microstructures in poly (methylmethacrylate) and poly (dimethylsiloxane) using femtosecond pulses for photonic and microfluidic applications," Appl. Opt. Vol. 49, 2475-2489, 2010.

K. L. N. Deepak, R. Kuladeep, and D. Narayana Rao, "Emission properties of femtosecond (fs) laser fabricated microstructures in Polystyrene (PS)," Opt. Commun. Vol. 284, 3070-3073, 2011.

K. L. N. Deepak, R. Kuladeep, S. Venugopal Rao, and D. Narayana Rao, "Luminescent microstructures in bulk and thin films of PMMA, PDMS, PVA,and PS fabricated using femtosecond direct writing technique," Chem. Phys. Lett. Vol.503, 57-60, 2011.

K. L. N. Deepak, R. Kuladeep, V. Praveen Kumar, S. Venugopal Rao, and D. Narayana Rao, "Spectroscopic investigations of femtosecond laser irradiated polystyrene and fabrication of microstructures," Opt. Commun.Vol. 284, 3074-3078, 2011.

K. L. N. Deepak, S. Venugopal Rao, and D. Narayana Rao, "Femtosecond laser-fabricated microstructures in bulk poly (methylmethacrylate) and poly (dimethylsiloxane) at 800 nm towards lab-on-a-chip applications," Pramana-J. Phys. Vol. 75, 1221-1232, 2010.

K. L. N. Deepak, S. Venugopal Rao, and D. Narayana Rao, **"**Femtosecond laser micro fabrication in polymers towards memory devices and microfluidic applications", Proc. of SPIE, 8190, 81900R-1, 2011.

K. L. N. Deepak, S. Venugopal Rao, and D. Narayana Rao, "Femtosecond Laser Direct Writing and Spectroscopic Characterization of Microstructures, Craters, and Gratings in Bulk/Thin Films of Polystyrene," AIP conf. Proc. 1391, 271-274, 2011.

K. L. N. Deepak, S. Venugopal Rao, and D. Narayana Rao," Effects of thermal treatment on femtosecond laser fabricated diffraction gratings in polystyrene," Appl. Surf. Sci. 257, 9299-9305, 2011.

K. L.N. Deepak, R. Kuladeep, S. Venugopal Rao, and D.Narayana Rao, "Studies on defect formation in femtosecond laser-irradiated PMMA and PDMS," Radiation effects and defects in solids, 67, 88-101, 2012..

K. M. Davis, K. Miura, N. Sugimoto, and K. Hirao, "Writing waveguides in glass with a femtosecond laser," Opt. Lett. Vol. 21(21), 1729–1731, 1996.

L. V. Keldysh, Soviet Physics JETP **20**, 1307, 1965.

M. Ams, G, D. Marshall, P. Dekker, Dubov, V. K. Mezentsev, I. Bennion, and M. J. Withford, "Investigation of ultrafast laser–photonic material interactions: challenges for directly written glass photonics," IEEE J. Sel. Top. Quant. Electron., Vol. 14(5), 1370-1381, 2008.

M. Ams, G. D. Marshall, P. Dekker, J. A. Piper, and M. J. Withford, "Ultrafast laser written active devices," *Laser Photonics Rev.* Vol. 3(6), pp. 535–544, 2009.

N. Sanner, O. Uteza, B. Bussiere, G. Coustillier, A. Leray, T. Itina, and M. Sentis,¨Measurement of femtosecond laser-induced damage and ablation thresholds in dielectrics,¨ *Appl Phys A,* Vol. 94, pp. 889-897, 2009.

N. Sanner, O. Uteza, B. Chimier, M. Sentis, P. Lassonde, F. Legare, and J. C. Kieffer, "Toward determinism in surface damaging of dielectrics using few-cycle laser pulses," Appl. Phys. Lett. 96, 071111, 2010.

N. V. Sidorov, M. N. Palatnikov, V. T. Gabrielyan, P. G. Chufyrev, and V. T. Kalinnikov, "Raman spectra and structural perfection of Normally Pure Lithium Niobate crystals," Inorganic Materials, Vol. 43, No. 1, 60-67, 2007.

R. R. Gattass, and E. Mazur, "Femtosecond laser micromachining in transparent materials," *Nat. Photonics* Vol. 2(4), pp. 219–225, 2008.

S. M. Kaczmarek, R. Jablonski, I. Pracka, M. Swirkowicz, J. Wojtkowska, S. Warchol, "Radiation Defects in $LiNbO_3$ Single Crystals Doped with Cr3+ Ions," Cryst. Res. Technol. Vol. **34**, 729–735, 1999.

S. M. Kostritskii, and P. Moretti, "Micro-Raman study of defect structure and phonon spectrum of He-ion implanted LiNbO3 waveguides," phys. Stat. Sol (c) Vol. 1, No. 11, 3126-3129, 2004.

S. Taccheo, G. Della Valle, R. Osellame, G. Cerullo, N. Chiodo, P. Laporta, O. Svelto, A. Killi, U. Morgner, M. Lederer, D. Kopf, "Er : Yb-doped waveguide laser fabricated by femtosecond laser pulses," Opt. Lett. Vol. 29, 2626-2628, 2004.

S. Venugopal Rao, T. Shuvan Prashant, K.L.N. Deepak, Surya P. Tewari, G. Manoj Kumar, and D. Narayana Rao, "Laser Direct Writing of Photonic Structures in X-cut Lithium Niobate using Femtosecond Pulses", Proc. of SPIE Vol. 8173 81730G-1, 2011.

Sung Chul Bae, Hyunjung Lee, Zhiqun Lin, and Steve Granick, "Chemical Imaging in a Surface Forces Apparatus: Confocal Raman Spectroscopy of Confined Poly(dimethylsiloxane)", Langmuir Vol. 21, 5685-5688, 2005.

Terenin AN. Photonics of Dye Molecules. Nauka:Leningrad, 1967.

V. Caciuc, A. V. Postnikov and G. Borstel, " Ab initio structure and zone-center phonons in LiNbO3," Phys. Rev. B Vol. 61 (13), 8806-8813, 2000.

Vera-Maria Graubner, Rainer Jordan, Oskar Nuyken, Bernhard Schnyder, Thomas Lippert, Rudiger Kotz, Alexander Wokaun, "Photochemical modification of Cross-Linked Poly(dimethylsiloxane) by irradiation at 172 nm," Macromolecules Vol. 37, 5936-5943, 2004.

W. C. Galley, and R. M. Purkey, Proc. Natl Acad. Sci. USA 67, 1116-1121, 1970.

Y. Shimotsuma, P. G. Kazansky, J. Qiu, and K. Hirao, "Self-organized nanogratings in glass irradiated by ultrashort light pulses," Phys. Rev. Lett. Vol. 91(24), 247405, 2003.

Y. Zhang, L. Guilbert, P. Bourson, K. Polgar, and M. D. Fontana, " Characterization of short range heterogeneties in sub-congruent lithium niobate by micro-Raman spectroscopy," J. Phys. Cond. Matter. Vol. 18, 957-963, 2006.

Y.L. Zhang, Q.-D. Chen, H. Xia, and H.-B. Sun, "Designable 3D nanofabrication by femtosecond laser direct writing," *Nano Today* Vol. 5(5), pp. 435–448, 2010.

Z. Nie, H. Lee, H. Yoo, Y. Lee, Y. Kim, K.-S. Lim, M. Lee, "Multilayered optical bit memory with a high signal-to-noise ratio in fluorescent polymethylmethacrylate," Appl. Phys. Lett. Vol. **94,** 111912, 2009.

Lakshmi Narayana Deepak Kallepalli He has obtained his B. S. Hons in Physics and M. S. Physics with specialization in Photonics from Sathya Sai University, Puttaparthy, India. He received his Ph. D. degree entitled "Laser Irradiation Effects in Polymers, Lithium Niobate Crystal and Applications in Photonics" under the supervision of Prof. D. Narayana Rao, School of Physics, University of Hyderabad, and Hyderabad, India in January 2012. Currently, he is working as postdoctoral researcher at Lasers, Plasmas et Procedes Photoniques (LP3) laboratory, CNRS-Universite Aix-Marseille, Marseille.

Narayana Rao Desai He is currently a Professor of Physics at the University of Hyderabad, obtained his Ph. D. in Physics from IIT Kanpur. He has been working in the field of lasers and nonlinear optics for the last three decades. He has published nearly 150 papers in international journals. His current interests are optical limiting, photonic crystals, femtosecond laser direct writing, spectral interferometry, NLO studies of organic, inorganic and semiconductor nanoparticles.